Indian Journal of Biochemistry & Biophysics
Vol. 62, August 2025, pp. 919-928
DOI: 10.56042/ijbb.v62i8.16065

Antagonists binding at 5-HT_3R_{AA}, 5-HT_3R_{AB} and 5-HT_3R_{AC} can potentially counteract nicotine binding

Kok Wai Lam[1], Malina Jasamai[1], Nor Azlan Nor Muhammad[2] & Nor Syafinaz Yaakob[1]*

[1]Centre for Drug and Herbal Development, Faculty of Pharmacy, Universiti Kebangsaan Malaysia, Jalan Raja Muda Abdul Aziz, Kuala Lumpur-50300, Malaysia

[2]Institute of Systems Biology, Universiti Kebangsaan Malaysia, Bangi, Selangor-43600, Malaysia

Received 03 January 2025; *revised 17 January 2025*

5-hydroxytryptamine (serotonin) subtype 3 receptor (5-HT_3R) is a promising target for drug addiction treatment due to its functional role and brain distribution. However, 5-HT_3R may be composed of different subunits which potentially lead to different ligand binding properties. This study aimed to construct an *in silico* model of human 5-HT_3R with distinct subunit compositions and to investigate its binding with ligands such as nicotine, compared to 5-HT_3R antagonists from both synthetic and natural sources. Homology models of 5-HT_3RAA, 5-HT_3RAB, and 5-HT_3RAC were developed using the murine 5-HT_3R crystal structure (4PIR) as a template. Docking studies with AutoDock assessed the binding properties of nicotine and several antagonists (ondansetron, palonosetron, 6-gingerol, and 6-shogaol) across different 5-HT_3R compositions. A radioligand binding assay on human 5-HT_3RAA characterized the binding affinities of each compound. *In silico* findings revealed that both homomeric and heteromeric receptors exhibited similar interactions with nicotine and the antagonists. Notably, nicotine, 6-gingerol, and 6-shogaol demonstrated less favorable binding energies compared to ondansetron and palonosetron, with nicotine showing the weakest affinity among all tested ligands *in vitro*. The study outcomes allow a prediction of nicotine action on 5-HT_3R as an antagonist, which can possibly be competed with other 5-HT_3R antagonists from different classes.This positions the 5-HT_3R as a viable target for pharmacotherapy in smoking cessation.

Keywords: 5-hydroxytryptamine (serotonin) subtype 3 receptor, 6-gingerol, 6-shogaol, Docking study, Homology models, Nicotine antagonists

Smoking is known to be a major global problem and has been shown to contribute to the increase in mortality rate due to the smoking related diseases such as respiratory problems, vascular diseases and cancer[1]. Currently, three pharmacological agents are commonly used in smoking cessation programs namely; nicotine replacement therapy (NRT), bupropion SR and varenicline[2]. Nicotine in NRT and varenicline are known to target nicotinic acetylcholine receptor (nAChR) while bupropion acts as a norepinephrine-dopamine reuptake inhibitor. However, there have been some side effects associated with these agents such as significant oral irritation for NRT[3], seizure risk for bupropion[4] and psychiatric problems for varenicline[5]. This urges a study on newer agents targeting new receptors to treat this addiction problem.

*Correspondence:
Phone: +60392897970;
Fax: +60326983271
E-mail: nsy@ukm.edu.my
Suppl. Data available on respective page of NOPR

Genetic studies have shown the association of genes encoding for 5-HT_3R with drug dependence such as alcohol[6,7] and nicotine[8,9]. Specifically for nicotine addiction, some associations between genes that coded for 5-HT_3A and 5-HT_3B subunits (HTR3A and HTR3B, respectively), and serotonin transporter (5-HTT) gene (SLC6A4) with nicotine dependence have been documented[9]. These genes have also been implicated in patients with comorbidities or multiple addictions like cocaine and alcohol addiction[8]. This finding is within expectation since 5-HT_3R_{AB} has been known to be expressed in the limbic area related to the neurobiology of nicotine addiction[10,11]. A previous review suggested that nicotine effects can be modulated by 5-HT_3R antagonists such as ondansetron and tropisetron in *in vitro*, *in vivo* and genetic study[12]. Therefore, this study attempted to gain insight into the possible mechanism where 5-HT_3R antagonists like ondansetron, palonosetron, 6-gingerol and 6-shogaol can potentially counteract the effect of nicotine at 5-HT_3R_{AA}, 5-HT_3R_{AB} and 5-HT_3R_{AC}. Ondansetron represents the first-generation 5-HT_3R antagonist

while palonosetron is the latest 5-HT_3R antagonist claimed to be superior in its efficacy; 6-gingerol and 6-shogaol are 5-HT_3R antagonist compounds from a natural source, *Zingiber officinale*. This study used computational methods (homology modelling, docking and molecular dynamics) and *in vitro* assay (radioligand binding) to investigate the binding properties of these ligands.

Materials and Methods

Sequence alignment

The sequence for human 5-HT3 subunit A (UniProtKB code: P46098), subunit B (UniProtKB code: O95264), subunit C (UniProtKB code: Q8WXA8) and template (PDB code: 4PIR) were downloaded from UniProtKB website[13]. Sequence alignment was done for all the sequences using the Clustal Omega software[14].

Homology modelling and validation

The template chosen for the homology modelling is 4PIR[15]which was downloaded from the Protein Data Bank (PDB). Based on this template, the homology model for 5-HT_3R_{AA}, 5-HT_3R_{AB} and 5-HT_3R_{AC} were built using MODELLER[16], Swiss Model[17]and I-Tasser[18]. For heteropentamer models, AABAB and AACAC stoichiometry were chosen based on the previous study[19]. Subsequently, all the homology models were validated by Ramachandran Plot[20], Verify3D[21] and ERRAT[22] whereall the model scores were compared with the template (4PIR) score.

Docking

Five ligands used in this study were nicotine, ondansetron, palonosetron, 6-gingerol and 6-shogaol (Fig. 1). These ligands were drawn using ChemDraw software and converted to 3D images using Chem3D software. Minimisation and short molecular dynamic simulation at 310K were introduced to reduce any steric clashes. The ligand format was changed from PDB to PDBQT using the AutoDock Tool. Important interacting residues such as ASP119, ASN123, THR174, THR176, TRP178, PHE221 TYR229 and GLU231 at principal loop together with TRP85, ARG87, TYR148, ASP199, SER201, VAL202, ASP64 and ILE66 at complementary loop were chosen to get the coordinate of orthosteric binding site by referring to the previous study[23]. Coordinate for docking procedure was used in AutoDockVina software[24]. Only ligand binding conformations with the most favourable binding energy were chosen for the binding interaction study.

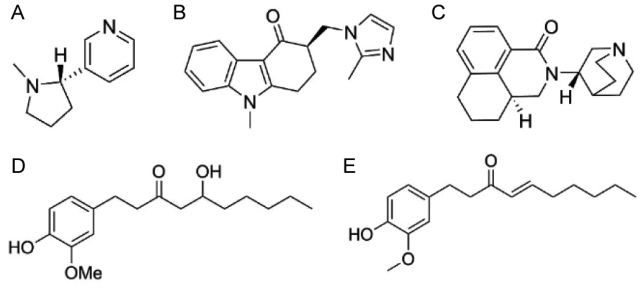

Fig. 1 — Chemical structures of (A) nicotine; (B) ondansetron; (C) palonosetron; (D) 6-gingerol; and (E) 6-shogaol

Molecular dynamic and MMPBSA analysis

The homology models were then uploaded to the Orientation of Protein Membrane website to orientate the model according to the template with accurate coordinates. Next, the orientated models were uploaded to the Charmm-GUI website[25] to prepare the model with 234 POPC lipids, 0.15M sodium chloride ions and water molecules as a complete system for molecular dynamic simulation (Fig. S1). CHARMM36m force field was chosen for this part[26]. The parameters for the simulation (potential energy, pressure and temperature) were observed to ensure that the systems are stable (Fig. S1 (A-D)).

Molecular dynamic simulation was carried out using the model to observe the binding energy predictions. Trajectory files (TRR files) from the simulation were used in the MMPBSA software[27]to get the binding energy reading. These TRR files were converted to compressed XTC files and only 250 frames were systematically extracted throughout the simulation. The findings were presented in the form of a line graph using the Grace software. MMPBSA evaluated protein and ligand binding energy in the solvent using the binding energy equation $\Delta G_{binding} = G_{complex} - (G_{protein} + G_{ligand})$ which is a product of protein energy and ligand energy subtracted from complex energy[28]. The same method was used to run simulations for equilibrated models.

Radioligand binding assay

The radioligand binding assay was carried out by referring to the protocol provided by the manufacturer. An assay buffer of 5mLwas used to dilute the 0.025mL membrane (1:500 dilution). Radioligand [3H]-GR65630 concentrations used for saturation assay are 0,0.027, 0.041, 0.061, 0.092, 0.138, 0.207, 0.310, 0.465, 0.698, 1.050, 1.570, 2.354, 3.521, 5.297, 7.945, 11.917(nM). For non-specific binding, 25 mL of incubation assay was used while

25 mL of 10 mM MDL72222 was used for specific binding. For competition binding assay, 25mL of competing compounds (nicotine, ondansetron, palonosetron and 6-gingerol) at decreasing concentrations (100 mM, 10 mM, 1 mM, 100 nM, 10 nM, 1 nM, 100 pM and 10 pM) were chosen to compete with 1nM of radioligands. The mixture was incubated for 60 min at 27°C. The excess solution was removed and ice-cold wash buffer (500 µL) was used to wash the grade GF/C microfibre filter paper presoaked with 0.05% polyethyleneimine (PEI). The liquid scintillation counter used is Tri-Carb 3110TR. The binding affinity of the competing ligands was calculated using the Cheng-Prusoff equation[29].

Results and Discussion

Sequence alignment and homology modelling of human 5-HT$_3$R$_{AA}$, 5-HT$_3$R$_{AB}$ and 5-HT$_3$R$_{AC}$

Sequence alignment showed that murine and human 5-HT$_3$R subunit sequences did not differ significantly based on their characteristics (Fig. 2). In terms of length, murine 5-HT$_3$A has 487 amino acids while human 5-HT$_3$A has 478 amino acids and murine 5-HT$_3$B has 437 amino acids while human 5-HT$_3$B has 441 amino acids[30]. Human 5-HT$_3$C with 447 residues cannot be compared with murine as rodents do not have subunit C[31].

Residues composition of subunits A, B and C vary at the regions of intracellular, extracellular, transmembrane and also at the ligand binding site. In previous reports comparing the 5-HT$_3$R$_A$ and 5-HT$_3$R$_{AB}$ receptors, these differences were known to affect more on the biophysical part of the receptors compared to the pharmacological properties[32,33]. This suggested that the differences are most likely to minimally affect the ligand binding at the receptor. Generally, both agonist and antagonist bind at the interface between A subunit for both homopentamer and heteropentamer[34]. However, the number of serotonin needed to activate 5-HT$_3$R$_{AA}$ could not be confirmed between 2 to 5[35].

The percentage of identity matrix of the human A subunit (P46098) is the highest which is 86.4% compared to the B subunit (O95264) (43.92%) and C subunit (Q8WXA8) (35.59%) when comparison was made to the 4PIR template. This is expected because the 4PIR template and P46098 sequences both consist of subunit A only (same subunit). In our study, 4PIR is still being used as the template to model subunits B and C since there is no crystal structure for 5-HT$_3$R$_{AB}$ and 5-HT$_3$R$_{AC}$ in the PDB. Previously, most studies used the nAChR template[36] before the discovery of 4PIR[15]in which nAChR showed a lower percentage of the identity matrix.

Homology models were built using MODELLER, Swiss Model and I-Tasser then three validation software namely Ramachandran Plot, Verify3D and also ERRAT were used to evaluate the quality of the homology models. Outcomes of these different approaches and validation strategies are provided in Supplementary Information (Table S2). Based on the satisfactory validation scores of Ramachandran Plot, ERRAT and also Verify3D, the 5-HT$_3$R homology model built by Swiss Model approach was used for further 5-HT$_3$R *in silico* study. Validation results for human 5-HT$_3$R$_{AB}$ and 5-HT$_3$R$_{AC}$ models showed good scores and were not much different from the template score for all three validation methods.

Superimposed critical residues at the ligand binding site between the A-A interface with A-B and B-A interface, showed that A-A, A-B and B-A had different residue properties (Fig. 3A & B). Corresponding residues from subunit B were also located quite distant from the binding site. Similar observations were also seen for 5-HT$_3$R$_{AC}$ (Fig. 3C & D). These differences might explain why 5-HT$_3$R orthosteric ligands of both agonist and antagonist prefer to bind at the A-A interface only even in the heteromers 5-HT$_3$R$_{AB}$ and 5-HT$_3$R$_{AC}$[34] as this interface was consistent regardless of the presence of adjacent different subunits (Fig. 4). For downstream studies, this study utilised the equilibrated model for all 5-HT$_3$R subunit combinations which showed better validation scores compared with the unequilibrated model. Comparison of molecular dynamics data for the equilibration is provided in Supplementary Information (S3).

Binding energy prediction of nicotine, ondansetron, palonosetron, 6-gingerol and 6-shogaol at 5-HT$_3$R$_{AA}$, 5-HT$_3$R$_{AB}$ and 5-HT$_3$R$_{AC}$

MMPBSA analysis evaluated binding energy throughout 10 ns molecular dynamic simulation. Binding energy from MMPBSA analysis was calculated based on electrostatic energy, Van der Waal energy and also solvation energy (both polar solvation energy and SASA energy)[28]. The finding showed that the binding energy for all ligands (nicotine, ondansetron, palonosetron, 6-gingerol and 6-shogaol) were not significantly different at 5-HT$_3$R homopentamer and heteropentamer (Fig. 5). Nicotine, 6-gingerol and 6-shogaol showed less favourable binding energy

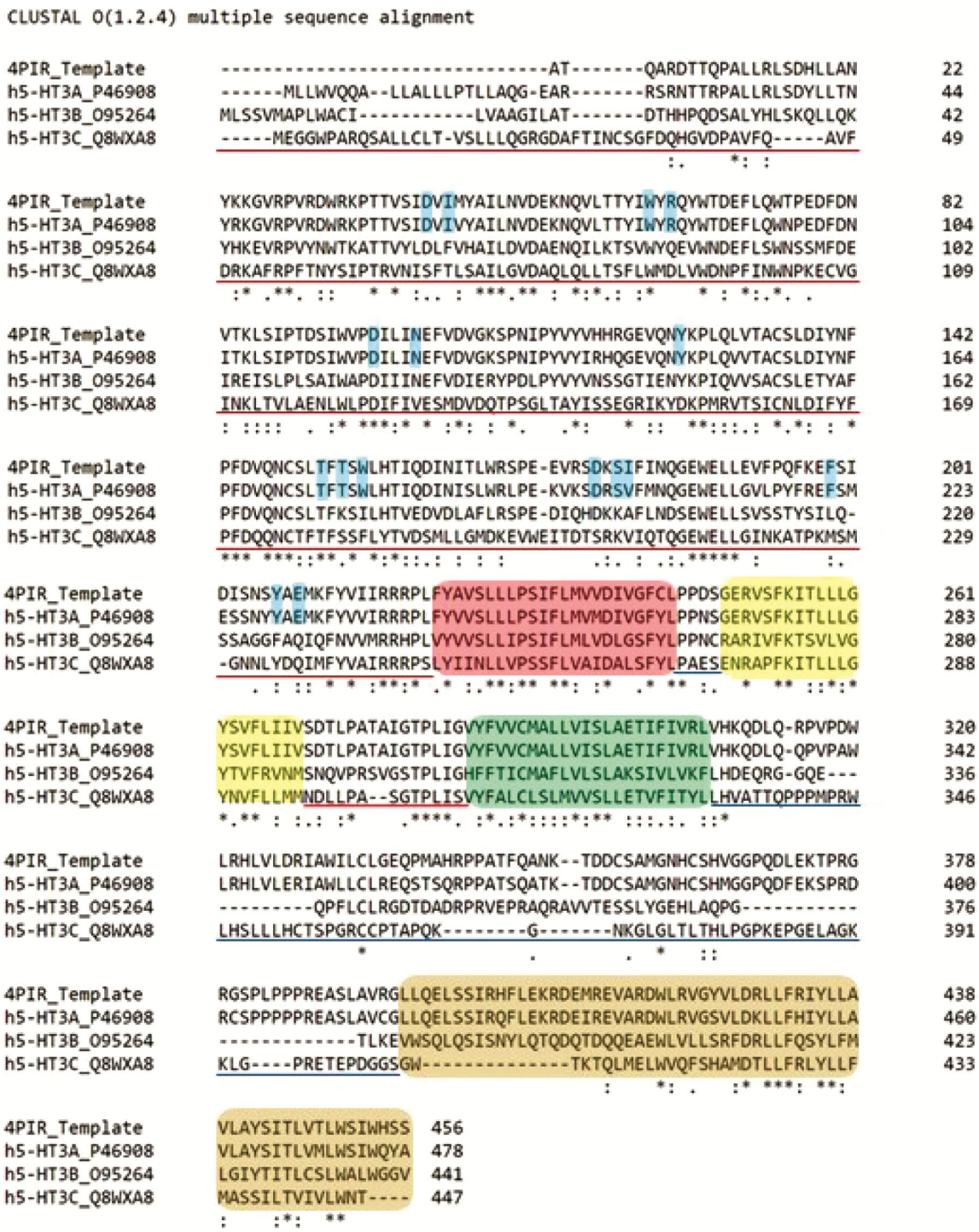

Fig. 2 — Sequence alignment of 4PIR, P46098, O95264 and Q8WXA8. Red line showed extracellular region while blue line referred to intracellular region. Residues from transmembrane 1, 2, 3 and 4 were coloured red, yellow, green and chocolate respectively while critical residues at the ligand binding site were blue-coloured

compared to ondansetron and palonosetron. This finding is supported by a previous study that reported the nicotine binding at 5-HT$_3$R is very weak[37]while 6-gingerol and 6-shogaol prefer to bind at allosteric binding site compared to the orthosteric binding site[38].

Ondansetron and palonosetron, being the 5-HT$_3$R conventional antagonists, showed very favorable binding energy at the orthosteric site of 5-HT$_3$R. This binding favorability was mostly contributed by electrostatic energy among others. Although in this

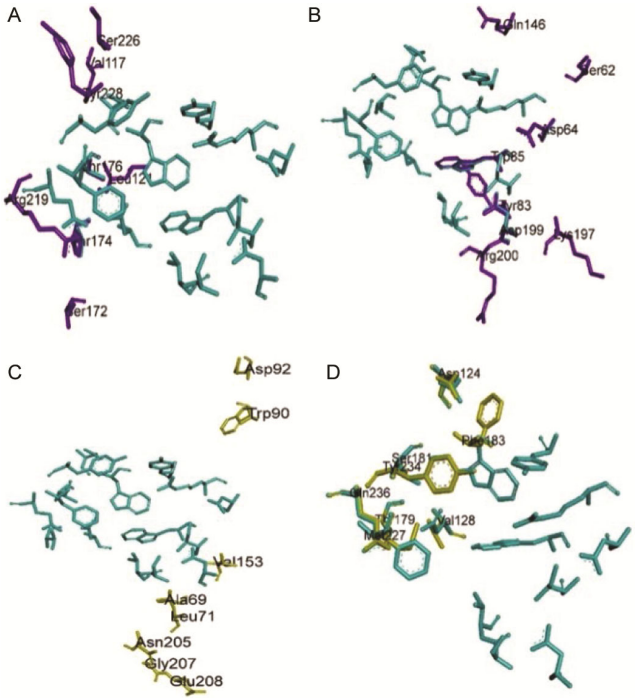

Fig. 3 — Critical residues at A-A interfaces superimposed with corresponding residues at (A) B-A, (B) A-B; (C) A-C; and (D) C-A interfaces

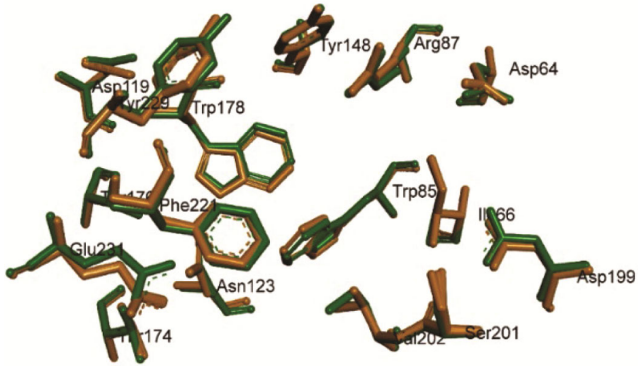

Fig. 4 — Critical residues at A-A interfaces from 5-HT_3R_{AA}, 5-HT_3R_{AB} and 5-HT_3R_{AC} (orange-coloured) were superimposed with critical residues at A-A interface from 4PIR (green-coloured)

prediction, ondansetron and palonosetron seem to have a very small difference most likely due to the model quality, previous study documented that palonosetron antagonises 5-HT_3R with very high affinity compared to ondansetron[39].

Interacting residues of 5-HT_3R and ligands

For the ligand interaction study, the last frame of the ligand and receptor were extracted from the simulation in order to analyse and compare the residue interactions for all ligands (nicotine, ondansetron, palonosetron, 6-gingerol and 6-shogaol) at 5-HT_3R_{AA}, 5-HT_3R_{AB} and 5-HT_3R_{AC}. The findings are summarised in (Table 1).

Eight residues showed important interactions with nicotine; TRP85, TYR86, ARG87, ASN123, TYR148, SER177, TRP178 and TYR229. Some of these residues were also shown to interact with other ligands. For example, ondansetron interacted with TRP85, ARG87, ASN123, TYR148, SER177 and TRP178, palonosetron interacted with TRP85, ARG87, ASN123, TYR148 and TRP178, 6-gingerol interacted with TRP85, TYR86, ARG87, ASN123, TYR148, SER177 and TRP178 and 6-shogaol interacted with TRP85, ARG87, ASN123, SER177 and TRP178. This binding interaction analysis showed that nicotine also shared binding residues with other 5-HT_3R ligands, despite weaker binding energy as previously described.

The binding conformation of the ligands at 5-HT_3R_{AA}, 5-HT_3R_{AB} and 5-HT_3R_{AC} were then superimposed to observe the binding favourability of the ligand at the binding site. For example, the binding conformations of ondansetron and palonosetron at all 5-HT_3R are very close to each other suggesting stable binding (Fig. 6B & C). At 5-HT_3R_{AC}, the tricyclic ring of ondansetron was facing slightly backwards compared to other binding conformation. Palonosetron binding conformation at 5-HT_3R_{AA} has quinuclidine ring facing just slightly frontwards and at 5-HT_3R_{AB} its tricyclic ring was a bit upwards. On the other hand, different binding conformation seen with nicotine, 6-gingerol and 6-shogaol suggesting unstable binding (Fig. 6A, D & E). Pyrrolidine ring of nicotine was facing left for 5-HT_3R_{AA}, right for 5-HT_3R_{AC} and upwards for 5-HT_3R_{AB}. This finding is slightly different from what has been reported by previous study where consistent binding conformation has been reported at nAChR and AChBP[40,41].

Furthermore, ligand RMSD values were observed to determine the binding stability throughout the simulation (Fig. 7A-C). This finding showed that the most unstable ligands at 5-HT_3R binding sites were 6-gingerol and 6-shogaol. At 5-HT_3R_{AA} binding site, 6-gingerol and 6-shogaol didn't achieve stability even after 10 ns. At 5-HT_3R_{AB}, 6-gingerol took around 8 ns to be stable while 6-shogaol needed 3 ns. This was somewhat expected since 6-gingerol and 6-shogaol were known to bind and antagonise 5-HT_3R but these two ligands were said to prefer to

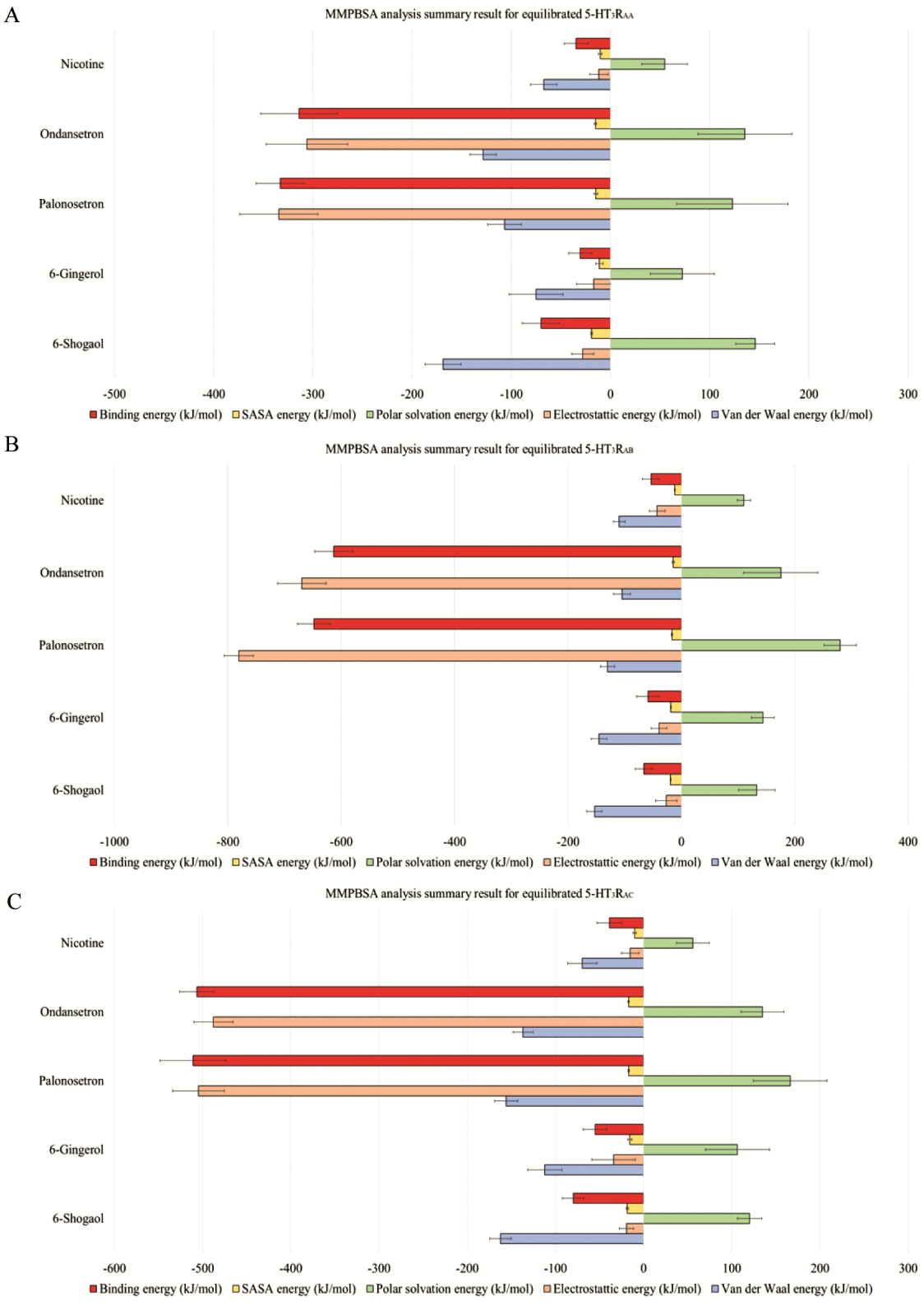

Fig. 5 — MMPBSA analysis summary result for equilibrated receptors (A) 5-HT_3R_{AA}; (B) 5-HT_3R_{AB}; and (C) 5-HT_3R_{AC}

Table 1 — Interacting residues of different ligands at 5-HT_3R_{AA}, 5-HT_3R_{AB} and 5-HT_3R_{AC}

Interacting residues	Ligands	5-HT_3R_{AA}	5-HT_3R_{AB}	5-HT_3R_{AC}
ILE66	ondansetron	/	/	nil
	palonosetron	/	/	/
	6-gingerol	nil	nil	nil
	6-shogaol	/	nil	nil
	nicotine	nil	nil	nil
TRP85	ondansetron	nil	nil	nil
	palonosetron	nil	/	/
	6-gingerol	nil	nil	/
	6-shogaol	/	/	nil
	nicotine	/	nil	/
ARG87	ondansetron	/	/	/
	palonosetron	/	/	nil
	6-gingerol	nil	/	/
	6-shogaol	/	nil	nil
	nicotine	nil	nil	nil
ASN123	ondansetron	nil	nil	/
	palonosetron	/	/	/
	6-gingerol	nil	/	nil
	6-shogaol	nil	/	/
	nicotine	/	nil	nil
TYR148	ondansetron	nil	nil	/
	palonosetron	nil	/	nil
	6-gingerol	/	nil	nil
	6-shogaol	nil	nil	nil
	nicotine	/	/	nil
TRP178	ondansetron	nil	/	nil
	palonosetron	nil	nil	/
	6-gingerol	/	/	/
	6-shogaol	nil	/	/
	nicotine	/	/	nil
VAL202	ondansetron	/	nil	nil
	palonosetron	nil	nil	/
	6-gingerol	nil	nil	nil
	6-shogaol	/	nil	nil
	nicotine	nil	nil	nil
SER177	ondansetron	nil	/	/
	palonosetron	nil	nil	nil
	6-gingerol	nil	nil	/
	6-shogaol	nil	/	nil
	nicotine	nil	/	nil
MET223	ondansetron	nil	/	/
	palonosetron	/	nil	/
	6-gingerol	/	nil	nil
	6-shogaol	nil	nil	/
	nicotine	nil	nil	nil
GLU231	ondansetron	/	/	/
	palonosetron	/	/	nil
	6-gingerol	nil	/	nil
	6-shogaol	/	nil	/
	nicotine	nil	nil	nil
PHE221	ondansetron	nil	/	nil
	palonosetron	nil	nil	nil
	6-gingerol	nil	/	nil
	6-shogaol	/	nil	/
	nicotine	nil	nil	nil
HR176	ondansetron	nil	/	/
	palonosetron	nil	nil	nil
	6-gingerol	nil	nil	/
	6-shogaol	nil	nil	nil
	nicotine	nil	nil	nil
TYR86	ondansetron	nil	nil	nil
	palonosetron	nil	nil	nil
	6-gingerol	nil	nil	/
	6-shogaol	nil	nil	nil
	nicotine	nil	nil	/
PRO150	ondansetron	nil	nil	/
GLU224	palonosetron	nil	/	nil
ARG87	nicotine	nil	/	/
TYR229	nicotine	/	/	/

*(/) mark signifies interaction present between a particular amino acid in the receptor and a particular ligand.

**(nil) signify absence of interaction between a particular amino acid in the receptor and a particular ligand.

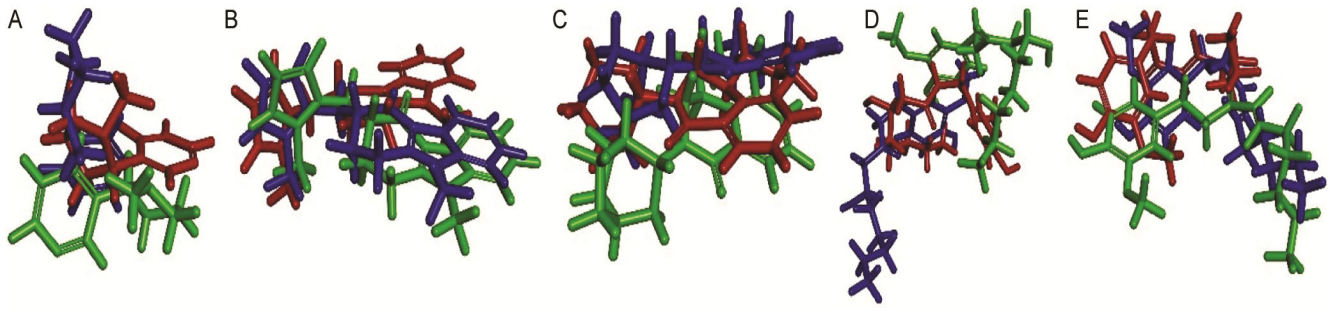

Fig. 6. Binding conformations of (A) nicotine; (B) ondansetron; (C) palonosetron; (D) 6-gingerol; and (E) 6-shogaol at 5-HT_3R_{AA} (green), 5-HT_3R_{AB} (blue) and 5-HT_3R_{AC} (red)

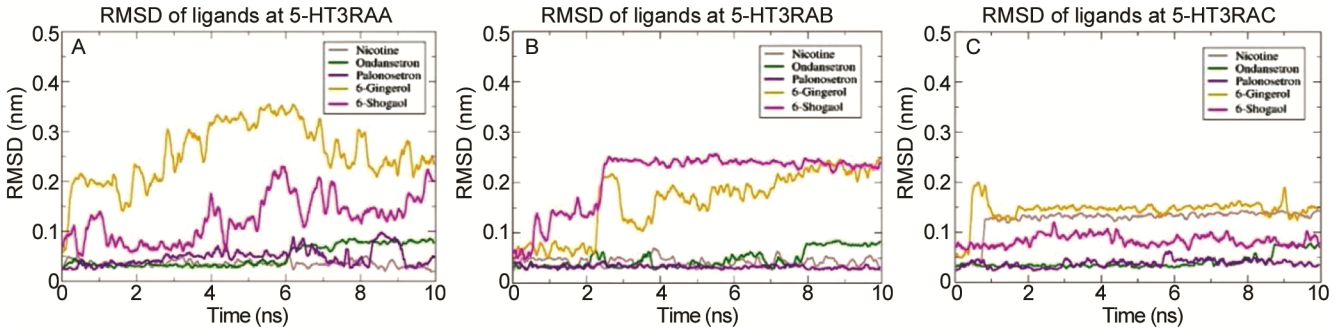

Fig. 7 — RMSD of ligands at (A) 5-HT$_3$R$_{AA}$; (B) 5-HT$_3$R$_{AB}$; and (C) 5-HT$_3$R$_{AC}$

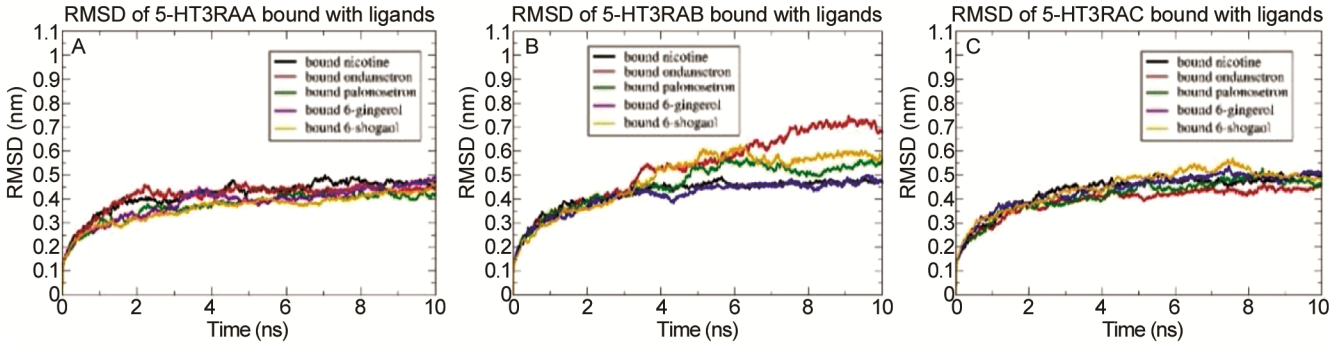

Fig. 8 — RMSD of different 5-HT$_3$R bound with ligands (A) 5-HT$_3$R$_{AA}$; (B) 5-HT$_3$R$_{AB}$; and (C) 5-HT$_3$R$_{AC}$

bind at the allosteric site compared to the orthosteric site[38]. At orthosteric binding site, aliphatic chain of 6-gingerol and 6-shogaol are expected to move a lot and unable to obtain a stable binding conformation. If further explanation on the binding properties of 6-gingerol and 6-shogaol is needed, visual conformation needed to be observed to extract the conformation at specific frame. Ondansetron on the other hand, throughout 10 ns its conformation changes very little to the more stable conformation with slight difference between the different receptor compositions *i.e.* 6ns at 5-HT$_3$R$_{AA}$, 8ns at 5-HT$_3$R$_{AB}$ and 9ns at 5-HT$_3$R$_{AC}$. In contrast, palonosetron and nicotine are very much stable along 10 ns with very minor RMSD value fluctuation.

Ligand RMSD of 5-HT$_3$R$_{AA}$, 5-HT$_3$R$_{AB}$ and 5-HT$_3$R$_{AC}$ were analysed to obtain the information regarding the receptor stability throughout the molecular dynamic simulation (Fig. 8A-C). RMSD of the receptor showed that different 5-HT$_3$R subunit such as A, B and C subunit influenced the stability of the receptor bound by the ligand once simulated using 10 ns molecular dynamic. It was obvious that 5-HT$_3$R$_{AA}$ and 5-HT$_3$R$_{AC}$ systems bound by ligands became stable easily in less than 2ns while 5-HT$_3$R consisted of subunit B, needed more time to be stable

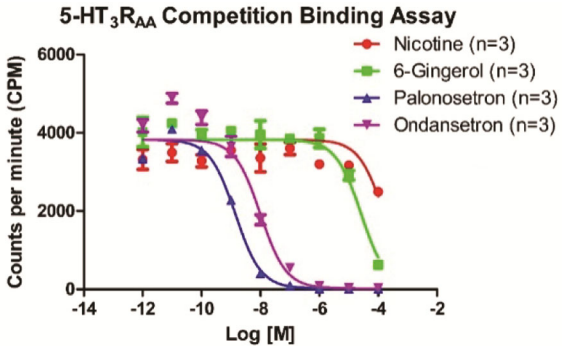

Fig. 9 — Radioligand competition binding assay usingmembrane expressing human 5-HT$_3$R$_A$

especially when bound to ondansetron, palonosetron and 6-shogaol. Overall, this showed that incorporation of subunit B but not C to form 5-HT$_3$R heteropentamer affect the stability of the receptor in molecular dynamic simulation, possibly the reason of different pharmacological properties observed of 5-HT$_3$R homopentamer and heteropentamer[32].

Binding affinity of 5-HT$_3$R ligands on 5-HT$_3$A receptor

Radioligand binding assay on membrane expressing human 5-HT$_3$R$_A$ indicated binding affinity properties and values of nicotine and 5-HT$_3$R antagonists as shown in (Fig. 9 and Table 2). Initial

Table 2 — Binding affinity of studied compounds

Compounds	Binding affinity (K_i)
Nicotine	66.33 mM
Ondansetron	4.09 nM
Palonosetron	0.57 nM
6-Gingerol	10.81 mM

saturation assay produced K_d and B_{max} values of 0.69 nM and 7679CPM (Fig. S4 and Table S4), respectively which conformed to the previously established reference control[42].

This finding suggested that nicotine competitively antagonise 5-HT_3R attheorthosteric binding site in agreement with the previous study[43,44] since at higher nicotine concentrations, the amount of bound radioligand was shown to be reduced. This is supported by another study where nicotine has been characterised to bind weakly at 5-HT_3R compared with other ligands[37]. K_i constant value of nicotine also was the highest compared to the ondansetron, palonosetron and 6-gingerol.

Palonosetron was shown to have the lowest K_i value at 0.57nM supporting that palonosetron is a very potent 5-HT_3R antagonist as reported by previous studies[33,39] followed by ondansetron, although a more recent study reported ondansetron inhibits 5-HT_{3A} receptor at 10-fold lower concentration than palonosetron[45]. On the other hand, 6-gingerol was known to bind allosterically[38]. Interestingly, in this study, 6-gingerol bound at the 5-HT_3R orthosteric site better than nicotine.

In summary, this study establishes a reliable homology model for the human 5-HT_3R using the 4PIR template. Our findings indicate that nicotine interacts with critical residues at the 5-HT_3R binding site but exhibits a weaker binding affinity compared to palonosetron and ondansetron. This is supported by the radioligand binding assay and MMPBSA analysis, which suggests that nicotine's low binding energy allows for potential displacement by ondansetron, palonosetron, 6-gingerol, and 6-shogaol. These results are relevant for both homomeric 5-HT_3R_A and heteromeric receptors (5-HT_3R_{AB} and 5-HT_3R_{AC}). Thus, one proposed mechanism for 5-HT_3R antagonists in modulating nicotine effects is through competitive displacement at the receptor site. Future research may also investigate the allosteric influence of 6-gingerol and 6-shogaol on nicotine binding. Overall, this study underscores the potential of 5-HT_3R antagonists as alternative treatments for nicotine dependence.

Acknowledgement

This work was primarily supported by a grant from the Universiti Kebangsaan Malaysia, Geran Galakan Penyelidik Muda (GGPM-2016-056).We would also like to acknowledge Muhammad Harith Zulkifli, Dr. Shuhaila Mat Shaarani, Genom Malaysia and Centre for Bioinformatics Research, Institute of Biology System, Universiti Kebangsaan Malaysia for providing the computer facilities (GUP-2018-147).

Conflict of Interest

All authors declare no conflicts of interest.

References

1 Collaborators GT, Spatial, temporal, and demographic patterns in prevalence of smoking tobacco use and attributable disease burden in 204 countries and territories, 1990-2019: a systematic analysis from the Global Burden of Disease Study 2019. *Lancet*, 397 (2021) 2337.

2 Giulietti F, Filipponi A, Rosettani G, Giordano P, Iacoacci C, Spannella F & Sarzani R, Pharmacological Approach to Smoking Cessation: An Updated Review for Daily Clinical Practice. *High Blood Press Cardiovasc Prev,* 27 (2020) 349.

3 Sivaramakrishnan G, AlsobaieiM & Sridharan K, Oral side effects of locally delivered nicotine replacement therapy: A meta-analysis of randomized controlled trials. *Int J Dent Hyg*, 21 (2023) 3.

4 Saffaei D, Lovett S & Rech MA, New-Onset Seizure in Patient Medicated With Bupropion for Smoking Cessation: A Case Report. *J Emerg Med,* 58 (2020) 145.

5 Menku B, Altiparmak T, Geniş B & Coşar B, Adverse Neuropsychiatric Events Associated with Varenicline: A Case Series. *Psychiat Behav Sci*, 11 (2021) 80.

6 Enoch MA, Gorodetsky E, Hodgkinson C, Roy A & Goldman D, Functional Genetic Variants that Increase Synaptic Serotonin and 5-HT3 Receptor Sensitivity Predict Alcohol and Drug Dependence. *Mol Psychiatr*, 16 (2011) 1139.

7 Seneviratne C, Franklin J, Beckett K, Ma JZ, Ait-Daoud N, Payne TJ, Johnson BA & Li MD, Association, interaction, and replication analysis of genes encoding serotonin transporter and 5-HT3 receptor subunits A and B in alcohol dependence. *Hum Genet*, 132 (2013) 1165.

8 Yang J & Li MD, Association and interaction analyses of 5-HT3 receptor and serotonin transporter genes with alcohol, cocaine, and nicotine dependence using the SAGE data. *Hum Genet*, 133 (2014) 905.

9 Yang Z, Seneviratne C, Wang S, Ma JZ, Payne TJ, Wang J & Li MD, Serotonin transporter and receptor genes significantly impact nicotine dependence through genetic interactions in both European American and African American smokers. *Drug Alcohol Depend*, 129 (2013) 217.

10 Davies PA, Pistis M, Hanna MC, Peters JA, Lambert JJ, Hales TG, Kirkness EF & Li MD, The 5-HT3B subunit is a major determinant of serotonin-receptor-function. *Nature*, 397 (1999) 359.

11 Gibbs E & Chakrapani S, Structure, Function and Physiology of 5-Hydroxytryptamine Receptors Subtype 3. *Subcell Biochem*, 96 (2021) 373.

12 Zulkifli MH, Viswenaden P, Jasamai M, Azmi N & Yaakob NS, Potential roles of 5-HT3 receptor (5-HT3R) antagonists in modulating the effects of nicotine. *Biomed Pharmacother*, 112 (2019) 112.

13 Consortium TU, UniProt: the Universal Protein Knowledgebase in 2023. *Nucleic Acids Res*, 51 (2022) D523.

14 Sievers F, Wilm A, Dineen D, Gibson TJ, Karplus K, Li W, Lopez R, Thompson JD, Higgins DG, McWilliam H, Remmert M & Soding J, Fast , scalable generation of high-quality protein multiple sequence alignments using Clustal Omega. *Mol Syst Biol*, 7 (2011) 1.

15 Hassaine G, Deluz C, Grasso L, Wyss R, Tol MB, Hovius R, Graff A, Stahlberg H, Tomizaki T, Desmyter A, Moreau C, Li XD, Poitevin F, Vogel H & Nury H, X-ray structure of the mouse serotonin 5-HT3 receptor. *Nature*, 512 (2014) 276.

16 Webb B & Sali A, Protein Structure Modeling with MODELLER. *Methods Mol Biol*, 2199 (2021) 239.

17 Waterhouse A, Bertoni M, Bienert S, Studer G, Tauriello G, Gumienny R, Heer FT, de Beer TAP, Rempfer C, Bordoli L, Lepore R & Schwede T, SWISS-MODEL: homology modelling of protein structures and complexes. *Nucleic Acids Res*, 46 (2018) W296.

18 Yang J & Zhang Y, Protein Structure and Function Prediction Using I-TASSER. *Curr Protoc Bioinformatics*, 52 (2015) 5.8.1.

19 Miles TF, Dougherty DA & Lester HA, The 5-HT3AB receptor shows an A3B2 stoichiometry at the plasma membrane. *Biophys J*, 105 (2013) 887.

20 Ramachandran S, Kota P, Ding F & Dokholyan VN, Automated Minimization of Steric Clashes in Protein Structures. *Proteins*, 79 (2011) 261.

21 Eisenberg D, Lüthy R & Bowie JU, VERIFY3D: assessment of protein models with three-dimensional profiles. *Methods Enzymol*, 277 (1997) 396.

22 Colovos C & Yeates TO, Verification of protein structures: Patterns of nonbonded atomic interactions. *Protein Sci*, 2 (1993) 1511.

23 Kesters D, Thompson AJ, Brams M, Van Elk R, Spurny R, Geitmann M, Villalgordo JM, Guskov A, Danielson UH, Lummis SCR, Smit AB & Ulens C, Structural basis of ligand recognition in 5-HT3 receptors. *EMBO Rep*, 14 (2013) 49.

24 Eberhardt J, Santos-Martins D, Tillack AF & Forli S, AutoDockVina 1.2.0: New Docking Methods, Expanded Force Field, and Python Bindings. *J Chem Inf Model*, 61 (2021) 3891.

25 Jo S, Kim T, Iyer VG & Im W, Software News and Updates CHARMM-GUI : A Web-Based Graphical User Interface for CHARMM. *J Comput Chem*, 29 (2008) 1859.

26 Huang J, Rauscher S, Nawrocki G, Ran T, Feig M, Groot DBL, Grubmuller H & Mackerell Jr AD, CHARMM36m: An Improved Force Field for Folded and Intrinsically Disordered Proteins. *Nat Methods*, 14 (2017) 71.

27 Valdés-Tresanco MS, Valdés-Tresanco ME, Valiente PA & Moreno E, gmx_MMPBSA: A New Tool to Perform End-State Free Energy Calculations with GROMACS. *J Chem Theory Comput*, 17 (2021) 6281.

28 Kumari R, Kumar R, Consortium OSDD & Lynn A, g_mmpbsa - A GROMACS Tool for High-Throughput MM-PBSA Calculations. *J Chem Inf Model*, 54 (2014) 1951.

29 Cheng YC & Prusoff WH, Relationship Between The Inhibition Constant (Ki) and The Concentration of Inhibitor Which Causes 50 Per Cent Inhibition (I50) of An Enzymatic Reaction. *Biochem Pharmacol*, 22 (1973) 3099.

30 Barnes NM, Hales TG, Lummis SCR & Peters JA, The 5-HT 3 receptor – the relationship between structure and function. *Neuropharmacology*, 56 (2009) 273.

31 Karnovsky AM, Gotow LF, McKinley DD, Piechan JL, Ruble CL, Mills CJ, Schellin KAB, Slightom JL, Fitzgerald LR, Benjamin CW & Roberds SL, A cluster of novel serotonin receptor 3-like genes on human chromosome 3. *Gene*, 319 (2003) 137.

32 Brady CA, Stanford IM, Ali I, Lin L, Williams JM, Dubin AE, Hope AG & Barnes NM, Pharmacological comparison of human homomeric 5-HT3A receptors versus heteromeric 5-HT3A/3B receptors. *Neuropharmacology*, 41 (2001) 282.

33 Thompson AJ & Lummis SCR, Discriminating between 5-HT3A and 5-HT3AB. *Br J Pharmacol*, 169 (2013) 736.

34 Lochner M & Lummis SCR, Agonists and Antagonists Bind to an A-A Interface in the Heteromeric 5-HT3AB Receptor. *Biophys J*, 98 (2010) 1494.

35 Rayes D, Spitzmaul G, Sine SM & Bouzat C, Single-Channel Kinetic Analysis of Chimeric α7 – 5HT3A Receptors. *Mol Pharmacol*, 68 (2005) 1475.

36 Unwin N, Refined Structure of the Nicotinic Acetylcholine Receptor at 4 A˚ Resolution. *J Mol Biol*, 346 (2005) 967.

37 Drisdel RC, Sharp D, Henderson T, Hales TG & Green WN, High Affinity Binding of Epibatidine to Serotonin Type 3 Receptors. *J Biol Chem*, 282 (2008) 9659.

38 Abdel-Aziz H, Windeck T, Ploch M & Verspohl EJ, Mode of action of gingerols and shogaols on 5-HT3 receptors: Binding studies, cation uptake by the receptor channel and contraction of isolated guinea-pig ileum. *Eur J Pharmacol*, 530 (2006) 136.

39 Wong EH, Clark R, Leung E, Loury D, Bonhaus DW, Jakeman L, Parnes H, Whiting RL & Eglen RM, The interaction of RS 25259-197, a potent and selective antagonist, with 5-HT3 receptors, *in vitro*. *Br J Pharmacol*, 114 (1995) 851.

40 Celie PHN, Rossum-fikkert VSE, Dijk VWJ, Brejc K, Smit AB, Sixma TK & Hepes A, Nicotine and Carbamylcholine Binding to Nicotinic Acetylcholine Receptors as Studied in AChBP Crystal Structures. *Neuron*, 41 (2004) 907.

41 Morales-perez CL, Noviello CM & Hibbs RE, X-ray structure of the human α4β2 nicotinic receptor. *Nature*, 538 (2016) 411.

42 Perkin E, Human Serotonin 5-HT3 Receptor. In: Technical Data Sheet Human Serotonin 5-HT3 Receptor (2019) 1.

43 Gurley DA & Lanthorn TH, Nicotinic agonists competitively antagonize serotonin at mouse 5-HT3 receptors expressed in Xenopus oocytes. *Neurosci Lett*, 247 (1998) 107.

44 Schreiner BSP, Lehmann R, Thiel U, Ziemba PM, Beltrán LR, Sherkheli MA, Jeanbourquin P, Hugi A, Werner M, Gisselmann Gn & Hatt H, Direct action and modulating effect of (+)- and (-)-nicotine on ion channels expressed in trigeminal sensory neurons. *Eur J Pharmacol*, 728 (2014) 48.

45 Basak S, Kumar A, Ramsey S, Gibbs E, Kapoor A, Filizola M & Chakrapani S, High-resolution structures of multiple 5-HT(3A)R-setron complexes reveal a novel mechanism of competitive inhibition. *Elife*, 9 (2020).